Available online at www.sciencedirect.com
SCIENCE DIRECT
Journal of Solid State Chemistry 179 (2006) 1035–1040
JOURNAL OF SOLID STATE CHEMISTRY
www.elsevier.com/locate/jssc

Synthesis, structure and physical properties of $GdCu_4Al$ and $GdCu_4Ga$

Svilen Bobev[a,*], Veronika Fritsch[b,1], Joe D. Thompson[b], John L. Sarrao[b]

[a]*Department of Chemistry and Biochemistry, University of Delaware, Newark, DE 19716, USA*
[b]*Materials Science and Technology Division MST-10, Los Alamos National Laboratory, Los Alamos, New Mexico 87545, USA*

Received 15 November 2005; received in revised form 18 December 2005; accepted 23 December 2005
Available online 27 January 2006

Abstract

Two non-stoichiometric Gd compounds, $GdCu_{5-x}Tr_x$ (Tr = Al, Ga) have been synthesized from the corresponding elements by high temperature reactions in sealed tantalum containers. They crystallize in the hexagonal $CaCu_5$-type (Pearson's symbol hP6, space group $P6/mmm$, No. 191) with lattice parameters determined from single-crystal X-ray diffraction at room temperature as follows: $a = 5.0831(10)$ Å; $c = 4.156(2)$ Å for $GdCu_{3.98(4)}Al_{1.02(4)}$, and $a = 5.1025(10)$ Å; $c = 4.155(2)$ Å for $GdCu_{3.9(1)}Ga_{1.1(1)}$, respectively. Structure refinements from single crystal X-ray diffraction data reveal that substitution of Cu for Al or Ga takes place preferably on one of the two transition metal sites with site symmetry mmm ($3g$). Both compounds order antiferromagnetically below ~40 K and ~36 K, respectively, as determined from temperature dependent dc-magnetization, resistivity and heat-capacity measurements.

Keywords: Rare-earth intermetallics; Crystal structure; Magnetic measurements; $GdCu_4Al$; $GdCu_4Ga$; AB_5-type intermetallics

1. Introduction

Binary Co-, Ni-, and Cu-rich rare-earth intermetallics have been extensively studied during the past 20–30 years due to their technologically important magnetic and hydrogen adsorption properties [1–3]. The steady interest in these materials has resulted in many papers, books and review articles, and the number of publications continues growing. Of particular appeal to us have been the $(RE)Cu_6$ binaries crystallizing with the orthorhombic $CeCu_6$ structure [4], as well as their ternary derivatives $(RE)Cu_{6-x}M_x$ (RE = *R*are *E*arth, M = Ag, Au, In), and the rich correlated-electron phenomenology they exhibit [5–8]. Very recently, other interesting physical properties, like geometrical frustration and first order valence transition were discovered in related $(RE)Cu_4Tr$ systems (Tr = Al, Ga, In), which are substitution variants of $(RE)Cu_5$ with the face-centered cubic $AuBe_5$ type [9–13]. Systematic experimental work on $(RE)Cu_4Tr$ showed that compounds with the early rare-earth metals (La–Sm) adopt the hexagonal $CaCu_5$ structure, whereas the compounds with late rare-earths (Ho–Lu) adopt the $AuBe_5$ structure [9]. With the mid-to-late rare-earths, largely depending on the experimental conditions, $(RE)Cu_4Tr$ compounds crystallize with either of the two possible structures. This confirms the trend that is well-established for the parent $(RE)Cu_5$ compounds [14].

With this paper, we report on the synthesis, structural characterization and the properties of two non-stoichiometric $GdCu_{3.98(4)}Al_{1.02(4)}$ and $GdCu_{3.9(1)}Ga_{1.1(1)}$ (for simplicity $GdCu_4Al$ and $GdCu_4Ga$ hereafter) ternary phases with the $CaCu_5$ structure [4]. The results presented herein confirm that substitution of Al and Ga for Cu causes significant changes in the magnetic and electrical properties compared to $GdCu_5$. However, in contrast with previous structural work [9,15,16], our refinements of the structure of $GdCu_4Al$ from single-crystal X-ray diffraction data indicate that the Cu–Al substitutions occur on only one of the two Cu sites. These results support the Reitveld analyses on the related heavy electron compounds $Ce(Cu_xAl_{1-x})_5$ and $Ce(Cu_xGa_{1-x})_5$ [17].

*Corresponding author. Fax: +1 302 831 6335.
E-mail address: sbobev@chem.udel.edu (S. Bobev).
[1]Present address: Physikalisches Institut, Universtät Karlsruhe, 76128 Karlsruhe, Germany.

0022-4596/$ - see front matter © 2005 Elsevier Inc. All rights reserved.
doi:10.1016/j.jssc.2005.12.034

2. Experimental

2.1. Synthesis

All manipulations of the pure elements were performed in an inert atmosphere or under vacuum. The starting materials Gd (Ames), Cu (Alfa), Al or Ga (Alfa-Puratronic), all with purity greater than 99.99% were used as received. Mixtures of these with the desired stoichiometric ratio of 1:4:1 were loaded in tantalum tubes, which were subsequently welded under argon atmosphere. The welded Ta-containers were then placed in fused silica ampoules, which were evacuated and flame-sealed. Reactions were carried out in a Lindberg muffle furnace at 1150 °C for 4 h, followed by cooling to 800 °C at a rate of −2 °C/h. At 800 °C the samples were removed from the furnace and allowed to cool to room temperature. The reaction outcome consisted of irregularly shaped crystals of golden color and up to a few millimetres in diameter. The crystals appear stable in air and moisture over periods of time greater than 6 months.

2.2. X-ray diffraction studies

X-ray powder diffraction patterns were taken on a Scintag XDS 2000 with monochromated Cu$K\alpha$ radiation ($\lambda = 1.5406$ Å). Powdered specimens were then placed on rotating sample holders, and powder X-ray diffraction data were taken up to a 2θ limit of 80°. The collected data were used for phase identification, which was done using the JADE 6.5 package [18]. All lines in the diffraction patterns could be indexed on basis of hexagonal cell with cell parameters ca. 5.1×4.15 Å, suggesting 95%+ phase purity.

To check and unequivocally establish the structure type and to verify the site occupancies for $GdCu_4Al$ and $GdCu_4Ga$, single crystals from both reactions were selected and mounted on the top of glass fibers (irregularly shaped, $0.05 \times 0.04 \times 0.03$ mm for $GdCu_4Al$, and $0.02 \times 0.01 \times 0.01$ mm for $GdCu_4Ga$, respectively). Intensity data were collected on a Bruker SMART CCD single-crystal diffractometer with monochromated Mo$K\alpha$ radiation at room temperature (0.4° ω scans, $2\theta_{max} = 58°$, full spheres). Data collections were done using the SMART software [19], and data reduction and integration was carried out with the aid of the SAINT package [20]. Semi-empirical absorption correction was applied based on SADABS [21]. $CaCu_5$ structure type was adopted as the structure model [9], and the structures were refined on F^2 with the aid of SHELXTL [22]. The refinements showed no indications that Gd in either structure is partially occupied. However, in the case of $GdCu_4Al$, when the Cu1 and Cu2 site occupancies were allowed to vary individually, deviations greater than 10σ were observed for Cu2, while the Cu1 site refined as full within 3σ. Therefore, in the final refinement cycles for $GdCu_4Al$, all occupation factors were kept at 100% with the Cu2 site ($M2$ hereafter) modeled as a statistical mixture of Cu and Al, which was refined as Cu/Al = 66.1(12)/33.9(12).

For $GdCu_4Ga$, because of the similar scattering factors of Cu and Ga, such analysis was not possible. Elemental analysis (below) on crystals from this batch confirmed the sample composition $GdCu_{3.9(1)}Ga_{1.1(1)}$, which is virtually identical with the refined composition for the Al-counterpart. Hence, in the final refinements for $GdCu_4Ga$, the model of $GdCu_4Al$ was used with Ga substitution for Cu on the Cu2 site only. Additional details of the data collection and structure refinements are given in Table 1. Positional and equivalent isotropic displacement parameters, and relevant interatomic distances are listed in Tables 2 and 3, respectively. Further details of the crystal structure investigations can be obtained from the Fachin-

Table 1
Selected single-crystal X-ray diffraction data collection and refinement parameters for $GdCu_4Al$ and $GdCu_4Ga$

Chemical formula	$GdCu_{3.98(4)}Al_{1.02(4)}$	$GdCu_{3.9(1)}Ga_{1.1(1)}$
Formula weight	438.39	481.75
Space group, Z	$P6/mmm$ (No. 191), 1	
Temperature	23(2) °C	
Unit cell parameters	$a = 5.0831(10)$ Å	$a = 5.1025(10)$ Å
	$c = 4.156(2)$ Å	$c = 4.155(2)$ Å
	$V = 92.99(4)$ Å^3	$V = 93.65(4)$ Å^3
Radiation, λ	Mo$K\alpha$, 0.71073 Å	
ρ_{calc}	7.828 g/cm^3	8.542 g/cm^3
2θ limit	54.8°	54.6°
Absorption coefficient	400.57 cm^{-1}	467.28 cm^{-1}
Collected/unique reflections	539/66	626/66
	[$R_{int} = 0.0184$]	[$R_{int} = 0.0256$]
Data/restraints/parameters	66/0/10	66/0/9
Goodness-of-fit on F^2	1.247	1.289
Final R indices ($I > 2\sigma_{(I)}$)[a]	$R_1 = 0.0203$	$R_1 = 0.0126$
	w$R_2 = 0.0436$	w$R_2 = 0.0314$
Extinction coefficient	0.049(6)	0.089(6)
Largest diff. peak and hole	+1.67/−0.82 e$^-$/Å^3	+0.71/−0.7 e$^-$/Å^3

[a] $R_1 = \sum||F_o|-|F_c||/\sum|F_o|$; w$R_2 = [\sum[w(F_o^2-F_c^2)^2]/\sum[w(F_o^2)^2]]^{1/2}$, and $w = 1/[\sigma^2F_o^2 + (AP)^2 + BP]$, $P = (F_o^2 + 2F_c^2)/3$; A and B—weight coefficients.

Table 2
Atomic coordinates, equivalent isotropic displacement parameters (U_{eq})[a] for $GdCu_4Al$ and $GdCu_4Ga$

Atom	Site	x	y	z	U_{eq} (Å^2)
$GdCu_4Al$					
Gd	1a	0	0	0	0.0126(5)
Cu(1)	2c	1/3	2/3	0	0.0137(6)
M(2)[b]	3g	1/2	0	1/2	0.0133(7)
$GdCu_4Ga$					
Gd	1a	0	0	0	0.0114(3)
Cu(1)	2c	1/3	2/3	0	0.0130(4)
M(2)[c]	3g	1/2	0	1/2	0.0119(4)

[a] U_{eq} is defined as one-third of the trace of the orthogonalized U_{ij} tensor.
[b] $M(2) = 66.1(12)\%$ Cu + 33.9(12)% Al—refined.
[c] $M(2) = 67\%$ Cu + 33% Ga—based on elemental analysis.

Table 3
Selected interatomic distances (Å) in $GdCu_4Al$ and $GdCu_4Ga$

$GdCu_4Al$		$GdCu_4Ga$	
Gd–6 × Cu1	2.9347(6)	Gd–6 × Cu1	2.9459(6)
Gd–12 × *M*2	3.2828(6)	Gd–12 × *M*2	3.2897(6)
Gd–2 × Gd	4.156(2)	Gd–2 × Gd	4.155(2)
Gd–6 × Gd	5.0831(10)	Gd–6 × Gd	5.1025(10)
Cu1–6 × *M*2	2.5437(7)	Cu1–6 × *M*2	2.5461(7)
Cu1–3 × Cu1	2.9347(6)	Cu1–3 × Cu1	2.9459(6)
Cu1–3 × Gd	2.9347(6)	Cu1–3 × Gd	2.9459(6)
*M*2–4 × Cu1	2.5437(7)	*M*2–4 × Cu1	2.5461(7)
*M*2–4 × *M*2	2.5416(5)	*M*2–4 × *M*2	2.5513(5)
*M*2–4 × Gd	3.2828(6)	*M*2–4 × Gd	3.2897(6)

formationszentrum Karlsruhe, 76344 Eggenstein-Leopoldshafen, Germany, (fax: (49) 7247-808-666; e-mail: crysdata@fiz.karlsruhe.de) on quoting the depository numbers: CSD 415940 ($GdCu_4Al$) and CSD 415941 ($GdCu_4Ga$).

2.3. Magnetic susceptibility measurements

Field-cooled dc magnetization measurements were performed in a Quantum Design MPMS-5 SQUID from 1.8 to 350 K in a magnetic field of 1 kG. Single crystals from $GdCu_4Al$ and $GdCu_4Ga$ were secured between pieces of quartz wool and suspended in a low background sample holder. Raw data were corrected for diamagnetic contribution from the holder and converted to magnetic susceptibility in emu/mol units.

2.4. Resistivity measurements

Measurements of the electrical resistivity as a function of the temperature were carried out in a custom built set-up using the four-probe technique from 1.3 to 300 K with excitation current of 1 mA. Due to the inability to find crystals with well-defined morphologies, we were unable to perform measurements in specific crystallographic directions. The data reported herein were taken on polished single crystals in order to minimize geometric and contact-resistance errors.

2.5. Calorimetry

Specific heat $C_p(T)$ data were obtained on a Quantum Design PPMS system using the thermal relaxation method in the temperature range 1.8–300 K.

2.6. Elemental analysis

Single crystals of $GdCu_4Ga$ were analyzed with a JEOL 7400F electron microscope equipped with an INCA-OXFORD energy-dispersive spectrometer. The microscope was operated at 10 μA beam current at 15 kV accelerating potential. The analysis resulted in a narrow range of totals—from 98% to 103%. From the data normalized per Gd, a ratio of Cu:Ga = 3.9(1):1.1(1) was established, which was used in the refinement of the single-crystal X-ray data in a manner consistent with the refinement on $GdCu_4Al$ (Table 2).

3. Results and discussion

$GdCu_4Al$ and $GdCu_4Ga$ crystallize with the ubiquitous $CaCu_5$ type (space group *P*6/*mmm*, No. 191—Fig. 1a). It is adopted by more than 400 binary, ternary and quaternary intermetallic compounds [9], and its important features have already been discussed elsewhere [1–3,14]. In this structure, there is only one unique site for the rare-earth metal atoms with symmetry of 6/*mmm* (Table 2). Hence, the Gd atoms form triangular layers perpendicular to the direction of the crystallographic *c*-axis (Fig. 1b), with

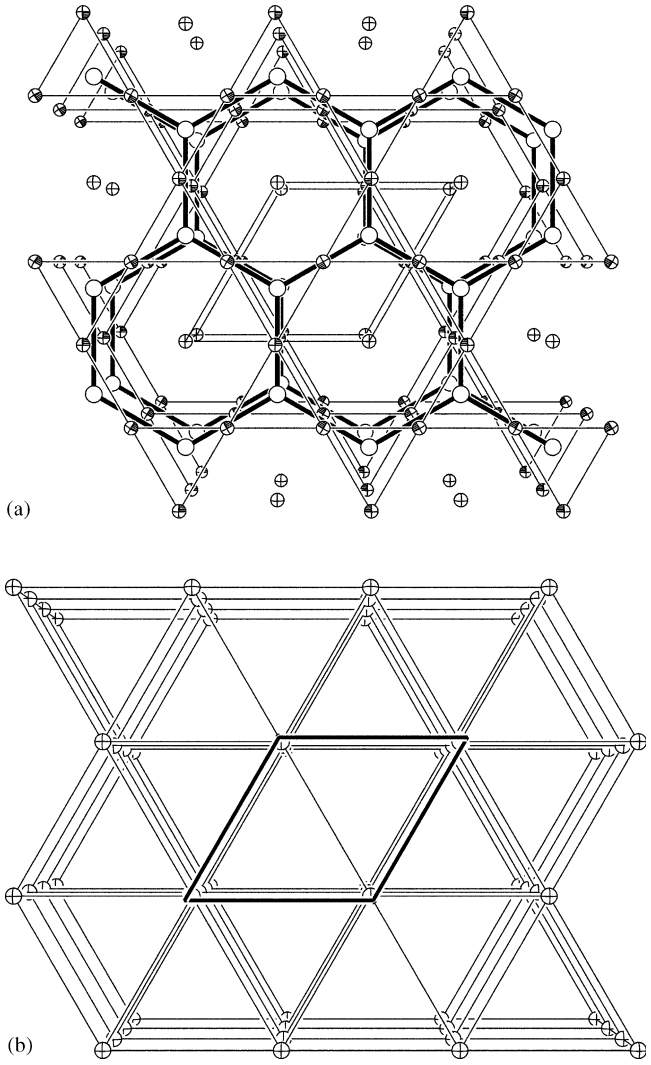

Fig. 1. (a) Perspective view of the hexagonal structure of $GdCu_4Al$ and $GdCu_4Ga$ ($CaCu_5$-type), viewed down the *c*-axis. Anisotropic displacement parameters are drawn at the 95% probability level: Gd atoms are shown with crossed ellipsoids, Cu1 is shown with empty circles and full ellipsoids represent the mixed Cu/Al sites (*M*2). (b) View of the Gd subnetwork only. Unit cell is outlined.

interlayer separation equal to the length of the *c*-axis and intralayer contacts equal to the length of the *a*-axis (Table 3). Evidently, the Gd–Gd interactions can be tuned by substituting Cu with another metal and thus changing the electron count and the magnitudes of both the *a*- and the *c*-axis. Such possibilities have been explored in the past, and there are several publications dealing with the variations in the magnetic properties upon formation of solid solutions, such as $GdCu_{5-x}Al_x$ ($0<x<2$) for example [15]. However, in almost all previous studies, attention has been paid only to the rare-earth sub-network and the substitution of *Tr*-elements on both Cu sites has not been analyzed beyond elemental analysis or expansion/contraction of the unit cell [15,16,23–25]. Indeed, for the composition ranges discussed herein, no refinements of the crystal structure have been done and equal distribution of Al on both Cu sites (2*c* and 3*g*—Table 2) has been assumed [16]. Our refinements on single-crystal data do not support such assignment—the results indicate that the Cu atoms (Cu1—Table 2), which are in the same plane with the Gd atoms (Fig. 2), cannot be exchanged with Al. Only the Cu atoms between the Gd sheets can be substituted as evidenced from the large deviations of the occupation factor. Although the refined occupancy (ca. 67:33) seems to suggest that one out of every three Cu atoms is substituted for Al, no presence of superstructure reflections was observed in the diffraction data. Structure refinements in lower symmetry were attempted but failed to support an ordered model for the Al substitution. These findings are supported by the Reitveld analyses from powder neutron diffraction on the related compounds $Ce(Cu_xAl_{1-x})_5$ and $Ce(Cu_xGa_{1-x})_5$ [17].

The corresponding Cu–Cu distances within one Cu-layer (pure Cu, located at $z=0$, Fig. 1) are 2.9347(6) Å in $GdCu_4Al$, and 2.9459(6) Å in $GdCu_4Ga$. The contacts within the mixed Cu/Al and Cu/Ga layers ($z=1/2$) are shorter—2.5416(5) Å in $GdCu_4Al$ and 2.5513(5) Å in $GdCu_4Ga$, respectively (Table 3). The interlayer Cu–Cu separations are in the same range—2.5437(7) Å in $GdCu_4Al$ and 2.5461(7) Å in $GdCu_4Ga$, respectively.

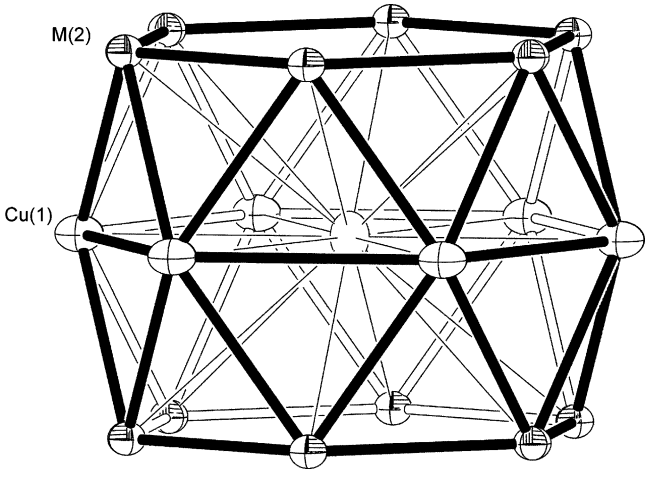

Fig. 2. Coordination polyhedron around the Gd atoms. Anisotropic displacement parameters are drawn at the 95% probability level: Gd atoms are shown with empty circles, Cu1 is shown with crossed ellipsoids and full ellipsoids represent the mixed Cu/Al sites (*M*2).

The Gd atoms have very high coordination number, 18, and the full coordination polyhedron is shown in Fig. 2. As discussed already, they form flat triangular layers perpendicular to the *c*-axis (Fig. 1b). Previous neutron diffraction studies on the binary $GdCu_5$ reveal incommensurate, helimagnetic-like magnetic structure along the *c*-axis—in each Gd layer, the Gd moments lie in layers in a frustrated arrangement, i.e. the interactions between nearest neighbors cannot be completely compensated [23]. This situation can be visualized as three Gd sub-lattices with an angle of 120° between each other and from layer to layer moments on the same *c*-axis at an angle of about 80° [23]. It has also been suggested that the energy of this triangular structure and the energy of the corresponding ferromagnetic one will be very close [15]. This hypothesis has been confirmed by field and temperature dependent susceptibility measurements on $GdCu_5$: an antiferromagnetic (AFM) order is seen below Néel temperature $T_N=26$ K but with positive Weiss temperature $\Theta_{CW}=7$ K and effective moment of 8.4 μ_B [23]. More recent study on $GdCu_5$ and on a series of $GdCu_{5-x}Al_x$ phases ($0<x<2$), prepared through arc-melting reports different parameters: much lower Néel temperature $T_N=12.5$ K and higher Weiss temperature $\Theta_{CW}=16.4$ K with effective moment of 8.5 μ_B [15]. This study shows that the magnetic interactions vary strongly, but not continuously with the Al content as concluded from the sudden jump of T_N around the phase with stoichiometry $GdCu_4Al$—reported are $T_N=45$ K, $\Theta_{CW}=-2.2$ K and an effective paramagnetic moment of 8.5 μ_B [15]. These data have been interpreted as a signature of transition from complex (almost ferromagnetic) state at low Al content ($0<x<1$) to apparently AFM state at higher Al content.

Our magnetic susceptibility $\chi=M/H$ vs. temperature T results on single crystals of $GdCu_4Al$ and $GdCu_4Ga$ prepared through different synthetic routes are in fair agreement with the earlier measurements on polycrystalline specimens [15]. A cusp-like feature is visible in the data (Fig. 3) at $T_N=40$ K for $GdCu_4Al$ and $T_N=36$ K for $GdCu_4Ga$, both determined from the mid-point in the jump in $d\chi/dT$, respectively. These peaks indicate the onset of long-range AFM order in both $GdCu_4Al$ and $GdCu_4Ga$. Given that the cell volume of $GdCu_4Ga$ is slightly larger than the cell volume of $GdCu_4Al$, it makes sense that the AFM order in the latter appears at slightly higher temperatures. Above T_N the inverse susceptibility increases linearly with the temperature indicating that the susceptibility follows the Curie–Weiss law, $\chi=C/T-\Theta_{CW}$, where C is the Curie constant and Θ_{CW} is the Weiss temperature. From the Curie constants the effective paramagnetic moments were calculated as follows: 8.27 μ_B for $GdCu_4Al$ and 8.6 μ_B for $GdCu_4Ga$. Both values are in agreement with the values for μ_{eff} from previous studies [15,23], but are somewhat higher than 7.94 μ_B,

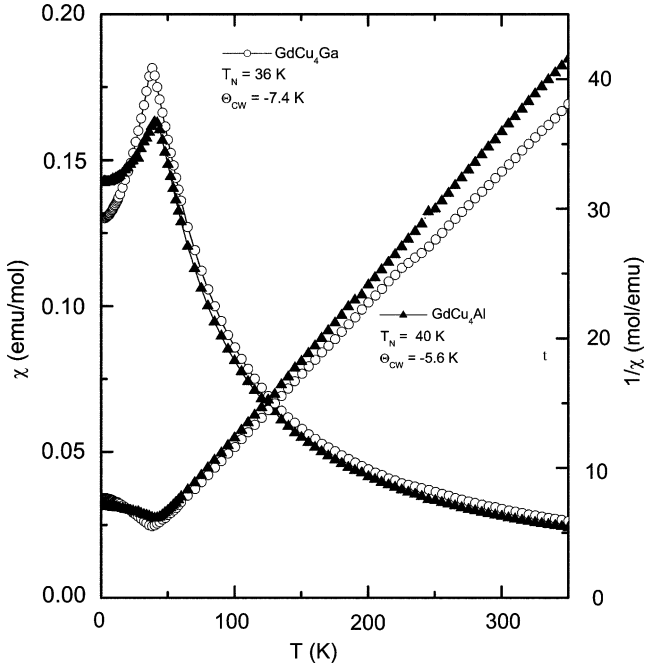

Fig. 3. Magnetic susceptibility $\chi(T)$ of $GdCu_4Ga$ and $GdCu_4Al$ (left axis). Right axis: inverse magnetic susceptibility ($\chi^{-1}(T)$) of $GdCu_4Ga$ and $GdCu_4Al$.

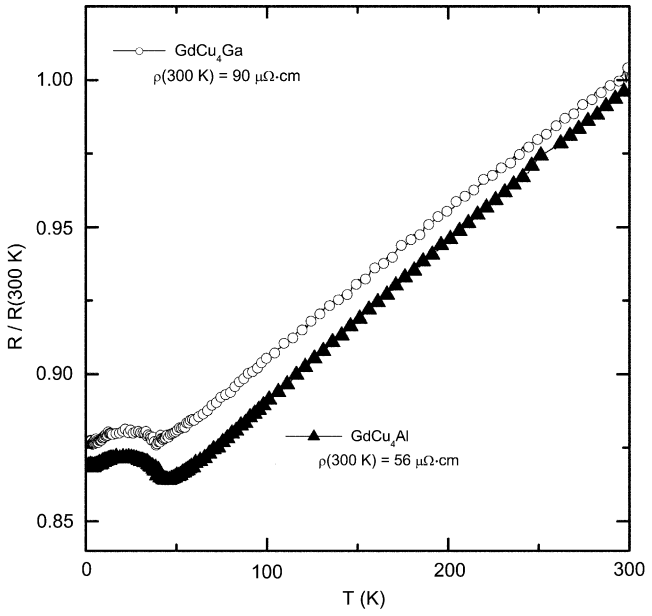

Fig. 4. Resistivity (ρ) as a function of temperature (T) of $GdCu_4Ga$ and $GdCu_4Al$, normalized on its value to 300 K.

which is the effective paramagnetic moment for free Gd^{3+} ions according to $\mu_{\text{eff}} = g[J(J+1)]^{1/2}$. This has been ascribed to a contribution from on-site $5d$ moments parallel to the local $4f$ moments [15]. The Weiss temperatures are negative for both compounds: $\Theta_{\text{CW}} = -5.6$ K for $GdCu_4Al$ and $\Theta_{\text{CW}} = -7.4$ K for $GdCu_4Ga$, respectively, as expected for antiferromagnets.

Fig. 4 shows the electrical resistivity of $GdCu_4Al$ and $GdCu_4Ga$ normalized on their values at 300 K. Above 50 K

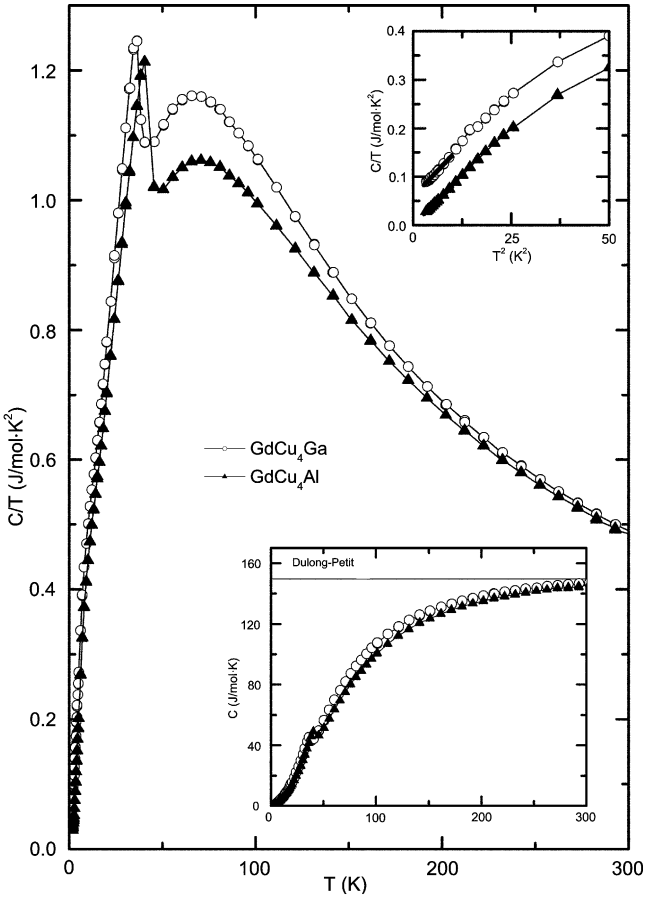

Fig. 5. Main frame: specific heat of $GdCu_4Ga$ and $GdCu_4Al$ in the representation C/T vs. T. Lower inset: specific heat of $GdCu_4Ga$ and $GdCu_4Al$ in the representation C vs. T. The solid line indicates the heat capacity expected after the law of Dulong and Petit. Upper inset: low temperature regime of the specific heat of $GdCu_4Ga$ and $GdCu_4Al$ in the representation C/T vs. T^2. The solid lines are linear fits assuming $C/T = \gamma + \beta T^2$.

the resistivities are linear, as it is expected for good metals. The resistivity at room temperature is $\rho_{300} = 56\,\mu\Omega\,\text{cm}$ for $GdCu_4Al$ and $\rho_{300} = 90\,\mu\Omega\,\text{cm}$ for $GdCu_4Ga$—about two orders of magnitude higher than the resistivities of pure noble metals. At $T = 45$ K for $GdCu_4Al$, and $T = 39$ K for $GdCu_4Ga$, respectively, the resistivities pass through V-shaped minima followed by broader maxima. These anomalies are certainly associated with the onset of AFM order, which was found at slightly lower temperatures by measurements of magnetic susceptibility and specific heat. The behavior of the resistivity in the magnetically ordered temperature regime is complex as is the magnetic structure (above). Slightly higher resistivity with similar temperature dependence has already been reported for arc-melted $GdCu_4Al$ [15]. The resistivity of the non-magnetic $LaCu_4Ga$ also shows quite similar linear behavior, and is of a similar magnitude [24].

Fig. 5 depicts the heat capacity (C) as a function of temperature for both $GdCu_4Al$ and $GdCu_4Ga$. The heat capacity of $GdCu_4Al$ and $GdCu_4Ga$ is illustrated in the

main frame in the representation C/T vs. T. In each measurement, a peak indicates the onset of AFM order, and the peak temperatures coincide nicely with the Néel temperatures found by susceptibility measurements (above). As it is shown in the lower inset of Fig. 5, the specific heat of both materials reaches a value of 150 J/mol K at high temperatures, which is in good agreement with the law of Dulong and Petit.

Estimated total entropy reached at the Néel temperature is in the order of 28 J/mol K for $GdAlCu_4$ and 26 J/mol K for $GdGaCu_4$. Since the entropy associated with the ordering of the Gd-moments is calculated to be $S_{magn.} = R\ln 8 = 17.3$ J/mol K, with R being the gas constant, that leaves entropy of about 10 J/mol K for lattice and electrons. This is a reasonable value for phonon and electron contribution, and compares well with the values obtained for the non-magnetic $LuCu_4In$ and $LuCu_4Cd$ for example—both have lattice entropy around 15 J/mol K at 40 K and for both the high temperature specific heat is approaching 150 J/mol K after the law of Dulong-Petit [27].

For conventional metals the heat capacity at low temperatures (roughly $T<\Theta_D/50$, where Θ_D is the Debye temperature) can be described as $C = \beta T^3 + \gamma T$, where βT^3 is the contribution of the phonons and γT is the contribution of the electrons to the specific heat, with γ being the Sommerfeld coefficient. Accordingly, if C/T vs. T^2 is plotted, as it is done in the upper inset of Fig. 5, one expects a linear behavior. The solid lines are linear fits to the data: $\Theta_D = 114$ K and $\gamma = 15$ mJ/mol K^2 for $GdCu_4Al$; $\Theta_D = 111$ K and $\gamma = 60$ mJ/mol K^2 for $GdCu_4Ga$. The values for both Debye temperatures are somewhat lower than the Debye temperature of the isostructural $LaCu_5$, for which $\Theta_D = 235$ K was found [26], whereas for $YbCu_4Al$, a Sommerfeld coefficient γ between 40 mJ/mol K^2 and 120 mJ/mol K^2 is reported [28]. The difference in the Sommerfeld coefficients of $GdCu_4Al$ and $GdCu_4Ga$ is probably due to differences in the DOS near the Fermi level—since the Sommerfeld coefficient is directly proportional to the DOS at the Fermi level; the difference between the Sommerfeld coefficients of $LuCu_4In$ and $LuCu_4Cd$ is also approximately a factor three [26].

4. Conclusions

We have reported a comprehensive structural and physical properties study of single crystals of $GdCu_4Al$ and $GdCu_4Ga$. Both compounds are substitution derivatives of $GdCu_5$ with the hexagonal $CaCu_5$ type. They order antiferromagnetically below 40 and 36 K, respectively. Refinements of single crystal X-ray diffraction data for $GdCu_4Al$ indicate preferred substitution of Cu with Al on one of the two crystallographic sites. The physical properties of the substituted $GdCu_{5-x}Tr_x$ analogs vary strongly, but not continuously with the Tr content and this may be a good starting point for the exploration of other transition metal substituted phases where the localized rare-earth spins form frustrated lattices.

Acknowledgments

Svilen Bobev acknowledges financial support from the University of Delaware through start-up funds. Work at LANL was performed under the auspices of the US DOE.

References

[1] K.A. Gschneidner Jr, L. Eyring (Eds.), Handbook on the Physics and Chemistry of Rare Earths, North-Holland, Amsterdam, 1979.
[2] A. Szytula, J. Leciejewicz (Eds.), Handbook of Crystal Structures and Magnetic Properties of Rare Earth Intermetallics, CRC Press, Boca Raton, FL, 1994.
[3] F.L. Schlapbach (Ed.), Hydrogen in Intermetallic Compounds, Springer, Berlin, Germany, 1988.
[4] D.T. Cromer, A.C. Larson, R.B. Roff Jr, Acta Cryst. 13 (1960) 913.
[5] G.R. Stewart, Rev. Mod. Phys. 56 (1984) 755.
[6] A. Germann, A.K. Nigam, J. Dutzi, A. Schroder, H. von Lohneysen, J. Phys. 49 (1988) 755.
[7] S. Bobev, E.D. Bauer, Acta Cryst. E 61 (2005) i79.
[8] S. Bobev, E.D. Bauer, Acta Cryst. E 61 (2005) i89.
[9] P. Villars, L.D. Calvert (Eds.), Pearson's Handbook of Crystallographic Data for Intermetallic Compounds, second ed., American Society for Metals, Materials Park, OH, 1991 and the desktop edition, 1997.
[10] V. Fritsch, J.D. Thompson, J.L. Sarrao, Phys. Rev. B 71 (2005) 132401.
[11] B.L. Young, N.J. Curro, V.A. Sidorov, J.D. Thompson, J.L. Sarrao, Phys. Rev. B 71 (2005) 224110.
[12] J.N. Hancock, T. McKnew, Z. Schlesinger, J.L. Sarrao, Z. Fisk. Phys. Rev. Lett. 92 (2005) 186405.
[13] I. Felner, I. Nowik, Phys. Rev. B 33 (1986) 617.
[14] K.H.J. Buschow, A.S. van der Goot, Acta Cryst. B 27 (1971) 1085.
[15] L.D. Tung, K.H.J. Buschow, J.J.M. Franse, P.E. Brommer, H.G.M. Dujin, E. Bruck, N.P. Thuy, J. Alloys Compds. 269 (1998) 17.
[16] T. Takeshita, S.K. Malik, W.E. Wallace, J. Solid State Chem. 23 (1978) 225.
[17] S.M. Kim, W.J.L. Buyers, H. Lin, E. Bauer, Z. Physik B: Cond. Mat. 84 (1991) 201.
[18] JADE Version 6.5, Materials Data, Inc., Livermore, CA, 2003.
[19] SMART NT Version 5.6, Bruker Analytical X-ray Systems, Inc., Madison, WI, 2003.
[20] SAINT NT Version 6.4, Bruker Analytical X-ray Systems, Inc., Madison, WI, 2003.
[21] SADABS NT Version 2.1, Bruker Analytical X-ray Systems, Inc., Madison, WI, 2001.
[22] SHELXTL Version 6.1, Bruker Analytical X-ray Systems, Inc., Madison, WI, 2001.
[23] J.M. Barandiaran, D. Gignoux, J. Rodrigez-Fernandez, D. Schmitt, Physica B 154 (1989) 293.
[24] E. Bauer, E. Gratz, N. Pillmayr, D. Gignoux, D. Schmitt, K. Winzer, J. Kohlmann, J. Magn. Magn. Mater. 76–7 (1988) 125.
[25] E. Bauer, N. Pillmayr, E. Gratz, D. Gignoux, D. Schmitt, K. Winzer, J. Kohlmann, J. Magn. Magn. Mater. 71 (1988) 311.
[26] V. Fritsch, J.D. Thompson, J.L. Sarrao, Phys. Rev. B (2005) submitted.
[27] M. Bouvier, P. Lethuillier, D. Schmitt, Phys. Rev. B 43 (1991) 13137.
[28] D.T. Adroja, S.K. Malik, B.D. Padalia, R. Vijayaraghavan, J. Phys. C: Solid State Phys. 20 (1987) L307.